Downloaded from orbit.dtu.dk on: Mar 17, 2025

DTU Library

Large eddy simulation of a premixed dual-fuel combustion: Effects of inhomogeneity level on auto-ignition of micro-pilot fuel

Nemati, Arash; Ong, Jiun Cai; Zhang, Min; Walther, Jens Honoré

Published in:
Fuel

Link to article, DOI:
10.1016/j.fuel.2023.128593

Publication date:
2023

Document Version
Publisher's PDF, also known as Version of record

Link back to DTU Orbit

Citation (APA):
Nemati, A., Ong, J. C., Zhang, M., & Walther, J. H. (2023). Large eddy simulation of a premixed dual-fuel combustion: Effects of inhomogeneity level on auto-ignition of micro-pilot fuel. *Fuel*, *349*, Article 128593. https://doi.org/10.1016/j.fuel.2023.128593

General rights
Copyright and moral rights for the publications made accessible in the public portal are retained by the authors and/or other copyright owners and it is a condition of accessing publications that users recognise and abide by the legal requirements associated with these rights.

- Users may download and print one copy of any publication from the public portal for the purpose of private study or research.
- You may not further distribute the material or use it for any profit-making activity or commercial gain
- You may freely distribute the URL identifying the publication in the public portal

If you believe that this document breaches copyright please contact us providing details, and we will remove access to the work immediately and investigate your claim.

Fuel 349 (2023) 128593

Contents lists available at ScienceDirect

Fuel

journal homepage: www.elsevier.com/locate/fuel

Full length article

Large eddy simulation of a premixed dual-fuel combustion: Effects of inhomogeneity level on auto-ignition of micro-pilot fuel

Arash Nemati [a,b,*], Jiun Cai Ong [a], Min Zhang [a,c], Jens Honoré Walther [a]

[a] Department of Civil and Mechanical Engineering, Technical University of Denmark, DK-2800 Kgs. Lyngby, Denmark
[b] Department of Energy Conversion and Storage, Technical University of Denmark, Fysikvej, DK-2800 Kgs. Lyngby, Denmark
[c] College of Engineering, Peking University, Beijing, 100871, PR China

ARTICLE INFO

Keywords:
Dual-fuel combustion
Inhomogeneity
Premixed methane
Micro-pilot diesel ignition
CFD simulation
LES

ABSTRACT

In a premixed dual-fuel (DF) methane-diesel engine, the ignition of the lean premixed methane/air mixture starts with the assistance of a pilot diesel injection. Auto-ignition of pilot fuel is important as it triggers the subsequent combustion processes. A delay in the auto-ignition process may lead to misfiring, incomplete combustion, and thus higher greenhouse emissions due to methane slip. Hence, a better understanding of the auto-ignition process for the pilot fuel can help to improve the overall engine performance, combustion efficiency, and to lower exhaust emission levels. In the present study, large eddy simulation (LES) is used to investigate the auto-ignition process of micro-pilot diesel in premixed DF combustion in a constant volume combustion chamber (CVCC). The entire DF combustion processes including methane gas injection, methane/air mixing, pilot diesel injection, and ignition are simulated. The numerical model is validated against experimental data. The present numerical model is able to capture the ignition delay time (IDT) within a maximum relative difference of 7% to the measurements. A higher relative difference of 38% is obtained when methane gas injection and mixing are omitted in the simulation and the methane/air is assumed homogeneous. This demonstrates the importance of inhomogeneity pockets. To study the effects of temperature and methane inhomogeneities separately, different idealized inhomogeneities in temperature and methane distribution are considered inside the CVCC. The inhomogeneity in the temperature is observed to have a more profound influence on the IDT than the methane inhomogeneity. The inhomogeneity pockets of temperature advance the first-stage ignition and, subsequently, the second-stage ignition. A sensitivity analysis on the effect of inhomogeneity wavelength reveals that the larger wavelengths enhance the combustion due to the presence of pilot diesel jets in the desirable regions for a longer time duration.

1. Introduction

Lean premixed combustion of natural gas (NG) in internal combustion engines is a promising alternative to diesel operation due to lower CO_2 emissions, significantly reduced particulate matter (e.g. soot), and less NO_x emissions [1]. However, the low chemical reactivity of NG leads to unreliable ignition and progression of combustion through lean mixtures. This results in a higher tendency of misfiring and combustion instability [2]. Therefore, highly reactive pilot fuel (e.g. diesel) is utilized to ensure stable and reliable combustion processes [3–11]. The amount of pilot diesel fuel is typically less than 20% of the total combined NG and diesel fuel energy content. If the diesel energy contribution goes below 5%, the combustion is referred to as a micro-pilot dual-fuel combustion [6].

In pilot fuel injection ignition systems, combustion is initiated by a small injection of a high-reactivity liquid fuel (typically diesel fuel) into a low-reactivity fuel-lean premixed charge of NG. The spatial and temporal occurrance of the auto-ignition sites are dependent on the physical mixing process between the pilot fuel and the premixed NG charge, as well as the chemical interactions between the two fuels. Prior optical investigations of diesel-piloted dual-fuel (DPDF) combustion were focused on measuring the ignition delay [9,10], flame luminosity [11], and the two-stage autoignition behavior of pilot fuel [7,8]. Furthermore, the influence of ambient methane (CH_4) concentration [3,7–9,11], ambient oxygen (O_2) level [5], ambient temperature [3,5,10,11], pilot fuel injection pressure [5,7–10], total injected pilot fuel mass [7–9,11], and number of pilot fuel injector holes [10] on the ignition and combustion processes of the DPDF system were investigated. It was observed that increasing of methane concentration in the air charge considerably prolongs the ignition delay [3,7–9,11]. Furthermore, increasing the pilot-fuel mass results in more complete combustion of

* Corresponding author at: Department of Civil and Mechanical Engineering, Technical University of Denmark, DK-2800 Kgs. Lyngby, Denmark.
E-mail addresses: arnem@dtu.dk (A. Nemati), jcong@dtu.dk (J.C. Ong), jhwa@dtu.dk (J.H. Walther).

https://doi.org/10.1016/j.fuel.2023.128593
Received 26 January 2023; Received in revised form 24 April 2023; Accepted 1 May 2023
Available online 24 May 2023
0016-2361/© 2023 The Author(s). Published by Elsevier Ltd. This is an open access article under the CC BY-NC license (http://creativecommons.org/licenses/by-nc/4.0/).

the premixed NG charge, but soot and NO_x emissions tend to increase. While, the combustion performance tends to deteriorate with lower pilot-fuel mass due to the high sensitivity of ignition delay to changes in premixed NG concentration [7–9,11].

In terms of numerical simulations, numerous studies [12–15] have been carried out to study the ignition and combustion process of DPDF combustion in a constant volume combustion chamber (CVCC). Wei et al. [12] and Zhao et al. [13] performed large eddy simulation (LES) of an n-heptane spray in a premixed methane/air environment under the Spray H condition from the ECN [16]. In addition, Kahila et al. [14] and Tekgul et al. [15] have performed numerical simulations to investigate the DF ignition process of an n-dodecane spray injection into a methane/air mixture. Their simulations were carried out in a CVCC under the Spray A condition from the ECN [16]. In all of the aforementioned numerical studies, the methane/air mixture is assumed to be fuel-lean and homogeneous. In general, the simulation results all demonstrate that the presence of methane increases the ignition delay time (IDT) of the injected pilot fuel. This is also in line with multiple experimental studies [3,7–9,11]. However, it is worth noting that none of the numerical studies above have validated their DPDF combustion results against measured data from a corresponding experimental setup.

Recently, Kilic et al. [17] performed numerical simulations of both diesel and DPDF combustion in a CVCC based on the experiment done by Yang et al. [6]. The numerical results were subsequently validated against the measured data in Ref. [6]. The simulated IDT for the DPDF combustion case was overpredicted. It was speculated that the overprediction may be attributed to the inhomogeneity in the premixed charge prior to pilot fuel injection. In this work [17], the methane/air mixture was assumed homogeneous. However, in the experiment methane gas is injected into the CVCC and allowed to mix with air for a period of time (~55 ms) prior to pilot fuel injection. Even using a port NG injection strategy, homogeneous NG/air mixture can only be achieved after 3 engine cycles as demonstrated in the optical experiment [7].

Despite having a homogeneous NG/air mixture, inhomogeneity may still be present in the mixture due to thermal stratification and turbulent structures in the bulk gas [7]. Meanwhile, it is shown in other experiments [1,11] that lowering the pilot diesel fuel mass (micro-pilot) could lead to large cycle-to-cycle variations and deterioration of combustion performance. This implies that when pilot fuel mass is low, the ignition process of the DPDF case is more sensitive to local inhomogeneities caused by thermal and mixture stratifications. To the authors' knowledge, the interaction between local inhomogeneities and the pilot fuel ignition process has not been studied previously.

Set against this background, the present study extends on our previous work [17] to investigate the effect of gas mixing and inhomogeneity on the ignition process of a micro-pilot dual-fuel combustion in a CVCC. The aim of the present work is achieved by performing LES of the full micro-pilot dual-fuel combustion process, including the direct injection of methane gas, mixing period of methane with air, pilot fuel injection, and finally ignition process of the micro pilot diesel jets. To understand the underlying mechanisms, different idealized inhomogeneities in temperature and methane distribution are considered in the same ranges that are observed in the simulated methane mixing process. Also, a sensitivity analysis is performed on the effect of the length scale (wavelength) of the inhomogeneities on the ignition process.

2. Case descriptions

The numerical simulations in the present study are based on the experiments performed by Yang et al. [6]. Full details of the experiments and procedure to achieve premixed diesel-methane DF combustion process in a CVCC are available in [6]. The experiment is carried out in an optically accessible 1.1 L cubic-shaped combustion chamber (Fig. 1). To mimic the thermodynamics and the flow conditions of a premixed DF engine using a CVCC, the following steps were taken in the experiment [6]. The standard pre-burn process was first conducted using a lean mixture of acetylene, hydrogen, oxygen, and nitrogen to generate a high-temperature mixture with the desired oxygen concentration. Methane gas was subsequently injected into the chamber for a duration of 25.8 ms and allowed to mix with air prior to the pilot diesel injection for approximately 55 ms. This was followed by the delivery of the pilot diesel fuel [6]. It should be mentioned that the 55 ms of mixing time corresponds to 360, 120, and 48 crank angle degrees of the heavy-duty engine (1200 rpm), medium-speed marine engine (400 rpm), and low-speed marine engine (160 rpm), respectively. Therefore, only a limited time is available for the mixing process to occur as compared to the compression process of the engine if the methane fuel is directly injected into the cylinder during the compression process.

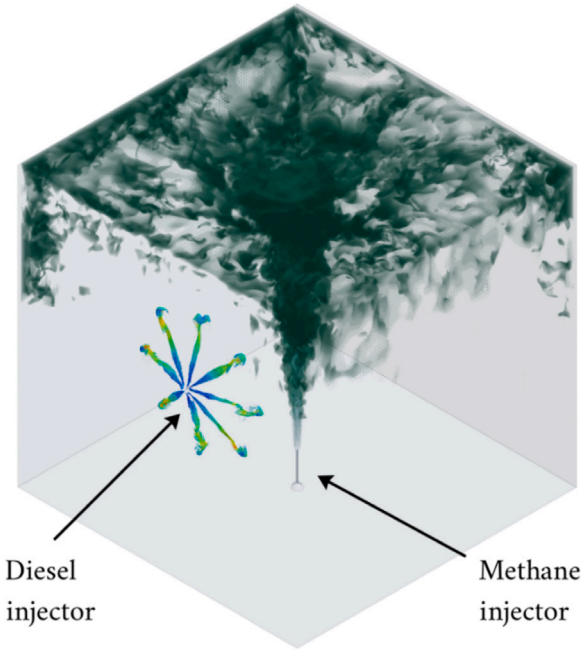

Fig. 1. Methane and diesel injections inside the constant volume combustion chamber.

In the experimental tests [6] and in the present LES study, pilot diesel fuel and methane fuel are delivered by two separate injectors. The location of these injectors are presented in Fig. 1. A single-hole gas injector with a nozzle hole diameter of 0.5 mm is used for methane injection with an injection duration and flow rate of 25.8 ms and 14.4 g/s, respectively. An 8-hole injector with nozzle hole diameters of 0.169 mm is used as the pilot diesel injector. The 8-holed diesel injector is located at l_{disp} = 11 mm and W = 51.6 mm from the wall boundaries, as depicted in Fig. 2. The injector holes are assumed to be equally distributed along a circle with a radius (r) of 1 mm. The included angle is 150° as depicted in Fig. 2. The injection pressure and injection duration for pilot diesel are set to 1000 bar and 0.25 ms, respectively. The total pilot diesel mass of 1.7 mg is injected into the CVCC similar to the experimental tests by Yang et al. [6]. This is equivalent to 1.6% diesel energy contribution and therefore qualifies as micro-pilot diesel (<5%) [6]. The fuel temperature for both diesel and methane are set to 300 K. The diesel fuel used in the experiment has a density of 784 kg/m^3 and a cetane number (CN) of 85 [6].

3. Numerical modeling

In the present study, 3-D CFD simulations are performed using the Siemens Star-CCM+ version 16.06.008-R8. Star-CCM+ is a multiphysics CFD software based on the finite volume method. The governing equations for the gas-phase flow are the filtered compressible Navier–Stokes equations which describe the conservation of mass, momentum, energy, and species [18,19]. An Eulerian–Lagrangian approach is used

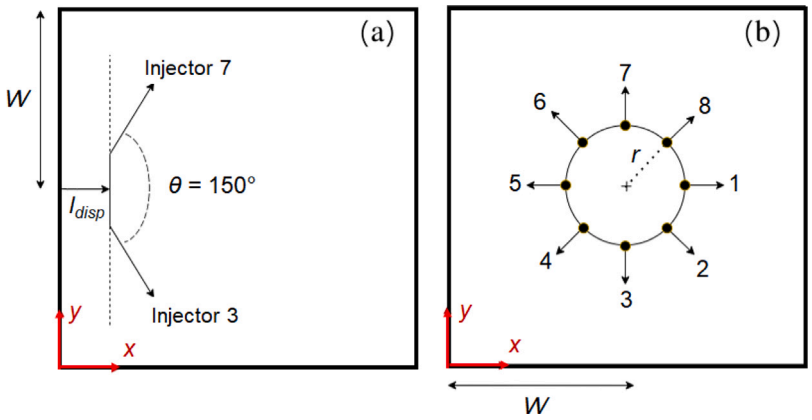

Fig. 2. Illustration of the combustion chamber geometry and the location of diesel injector nozzle holes: (a) cross-sectional view and (b) top view.

within the LES framework to model the fuel spray, gas flow, and combustion processes [20,21]. The sub-grid scale is described by the dynamic Smagorinsky model [22,23]. The primary breakup of diesel spray is considered by sampling computational parcels from the Rosin–Rammler size distribution. The secondary spray breakup is modeled by the Reitz–Diwakar breakup model [24,25]. The well-stirred reactor (WSR) model is used in the current LES, assuming no turbulence-chemistry interactions. The WSR model has been extensively used in other spray combustion studies [14]. In this study, n-dodecane ($C_{12}H_{26}$) fuel is employed as a surrogate for the diesel fuel used in the experiment [6]. The cetane number (CN) of $C_{12}H_{26}$ matches the CN of diesel fuel used in the experiments. The skeletal n-dodecane mechanism developed by Lapointe et al. [26] is used in this work. Performance of the Lapointe mechanism is evaluated by validation of predicted IDT and laminar flame speed in a 0-D homogeneous reactor model in our previous work [17].

The computational domain is a cubic chamber with side length of 103.2 mm, which corresponds to the 1.1 L combustion vessel in the experiment [6]. The side length of 103.2 mm is relevant to the piston bowl diameter of 72 mm of a Cummins ISB 6.7 L engine which is modified for micro-pilot dual-fuel operation by Naber et al. [27]. The initial ambient density and temperature prior to the start of methane injection are set to 13 kg/m^3 and 885 K, respectively. All boundaries are set as no-slip walls with Neumann boundary conditions for the ambient mixture composition and pressure. The temperature of the walls is set to 350 K.

Adaptive mesh refinement (AMR) is implemented in the present work. This is to ensure that the regions of interest have a cell size that is sufficiently small to capture the flow physics and combustion characteristics. A base mesh size of 1 mm and a minimum mesh size of 0.25 mm are considered in the current AMR. For non-reacting flow, the velocity magnitude of the jet and mass fraction of fuel (methane or diesel) are used as criteria for refining the cells. For reacting flow, the mass fraction of OH radical is also considered with the aforementioned criteria for AMR. A cross-sectional view of the mesh is presented in our previous study [17]. The quality of the mesh is assessed using the LES quality index proposed by Celik et al. [28]. The method is expressed as a non-linear function of the viscosity and the modeled turbulent viscosity.

$$QI_{\mathrm{LES}} = \frac{1}{1 + 0.05(\nu_{\mathrm{t,eff}}/\nu)^{0.53}} \tag{1}$$

where, $\nu_{\mathrm{t,eff}}$ is the effective viscosity (laminar + turbulent) and ν is the molecular viscosity. The larger the modeled viscosity, the lower the quality criteria. According to Celik et al. [28], an average QI_{LES} value above 80% is reasonable for the quality of LES mesh. The average LES quality index in the whole diesel spray region (Fig. 3) is 86% during diesel injection which is above the threshold of 80% proposed by Celik et al. [28]. The count of computational cells at the start of methane mixing process is around 1 M cells which gradually increases to around 80 M cells at the end of mixing process before pilot diesel injection.

Adaptive time-stepping is implemented in all of the simulations to speed-up the computations. In the reacting case during the pilot diesel injection and combustion, the minimum time-step and maximum Courant number are set to 25 ns and 0.3, respectively. During the non-reacting methane injection process, the minimum time-step and maximum Courant number are set to 250 ns and 4, respectively. In the gas mixing process, both the spatial and temporal terms are discretized by second-order schemes.

4. Results and discussion

4.1. Validation of non-reacting spray

In this section, the characteristics of non-reacting methane and pilot diesel injections are validated with the available experimental data [6]. Fig. 4 shows the numerical and measured average pressure (P_{av}) of the CVCC during the injection and mixing of methane fuel. As it can be seen in Fig. 4, a reasonable agreement is achieved between the predicted P_{av} and the measurement [6]. During the methane mixing period, P_{av} decreases due to the heat losses from the walls. It should be mentioned that in the experimental study [6], the temperature of the combustion chamber was estimated using the pressure data. The temperature of the combustion chamber was determined using pressure, density, mixture molecular weight, and ideal gas law [6]. Therefore, validating the average pressure of CVCC helps to ensure accurate prediction of the correct average temperature of the combustion chamber prior to the pilot diesel fuel injection. This temperature has a critical effect on IDT and on the simulation of the auto-ignition process of the micro-pilot diesel fuel. For example, it is shown in an experimental study by Srna et al. [29] that in a methane-air ambient with a methane equivalence ratio of 0.5, by decreasing the average temperature from 850 K to 770 K, IDT of diesel increases by 50% (from ~1.0 ms to ~1.5 ms) under their studied operating condition [29].

Before considering the reacting case, the liquid penetration length (LPL) of the diesel injection is validated for the non-reacting case. LPL is defined here as the maximum axial distance encompassing 95% of the liquid fuel mass. In the non-reacting case, pilot diesel is injected into pure N_2 with an ambient temperature (T_{am}) of 453 K and ambient density (ρ_{am}) of 13 kg/m^3. Fig. 5 presents a comparison of numerical and experimental LPL of the non-reacting pilot diesel spray injection. Fig. 5 indicates that the numerical setup is able to capture the non-reacting pilot diesel spray characteristics.

Distribution of equivalence ratio (ϕ) as an indicator of methane fuel distribution and temperature inside the CVCC before the pilot diesel start of injection (SOI) are presented in Fig. 6. The distributions are

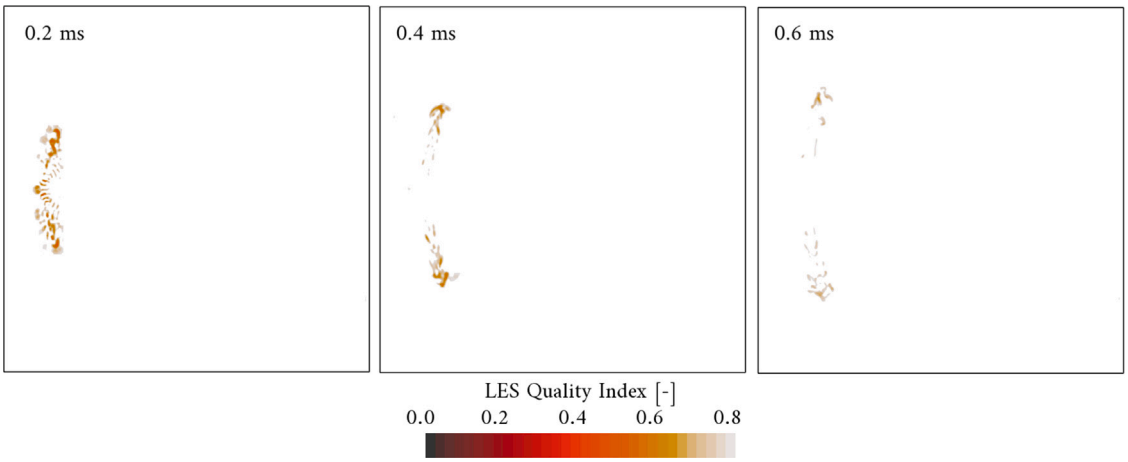

Fig. 3. Spatial distribution of LES quality index [28] at three different time instances after the start of pilot diesel injection.

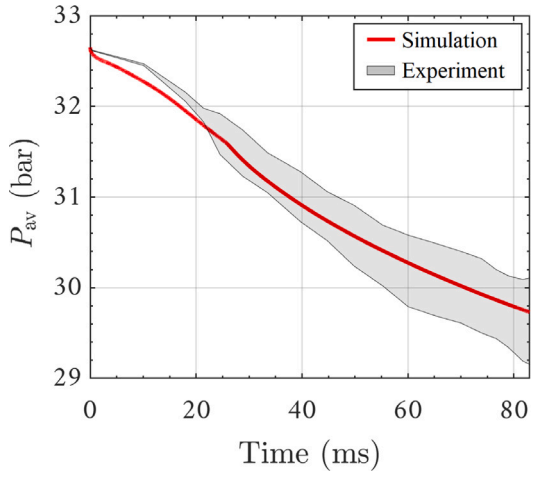

Fig. 4. Comparison of numerical and experimental [6] average pressure (P_{av}) of the constant volume combustion chamber during methane injection and mixing as a function of time after the start of pilot diesel injection. The gray shaded area specifies the error bar of the measured pressure.

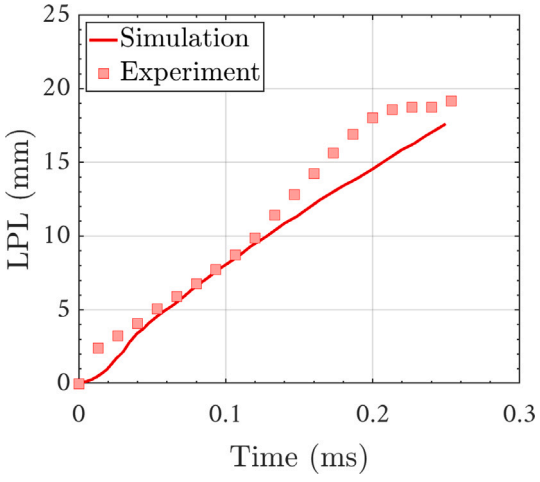

Fig. 5. Comparison of numerical and experimental [6] liquid penetration length (LPL) as a function of time after the start of pilot diesel injection.

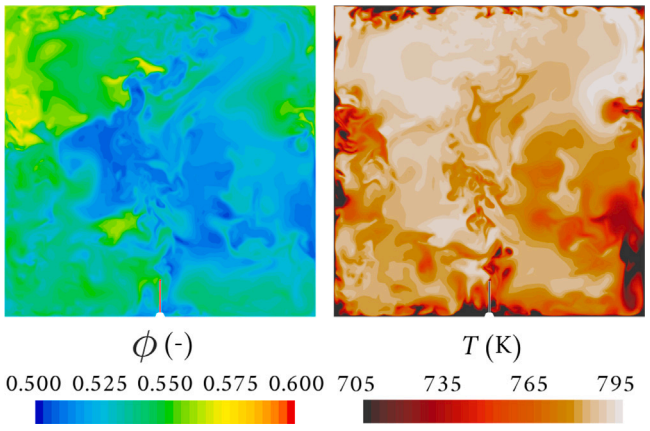

Fig. 6. Distributions of methane equivalence ratio (ϕ) and temperature (T) inside the constant volume combustion chamber before the start of pilot diesel injection.

presented on a cross-sectional plane passing through the methane and diesel injectors. This figure shows pockets of inhomogeneity in both the equivalence ratio and temperature distributions. The range of local temperature is around 705–795 K (cf. Fig. 6) which corresponds to a temperature variation of around 45 K from the reported average of 750 K. The equivalence ratio is in the range of 0.5–0.6 which corresponds to 8–12% variation in the local methane concentration from the reported average value of 0.54. The effects of inhomogeneity pockets on the auto-ignition of the pilot diesel will be studied in the following sections.

4.2. Validation of reacting spray

In this section, the ignition process of the pilot diesel fuel is studied in the methane/air environment which is simulated in Section 4.1. Validation of the reacting spray simulation is carried out by comparing the computed IDT with the measured IDT. The measured IDT is defined as the time between the start of the diesel injector hydraulic opening time and the first frame that diesel auto-ignition is identified in Schlieren images [6].

Three different definitions of IDT are considered for the 3-D CFD simulations: (1) the time taken for the mixture temperature to increase above 2000 K, (T_{max} > 2000 K), (2) the time when the greatest rise of the temperature is observed, $((dT/dt)_{max})$, and (3) the time when the greatest rise of the OH concentration is observed $((d[OH]/dt)_{max})$ [30]. The difference between the calculated IDTs is not considerable and

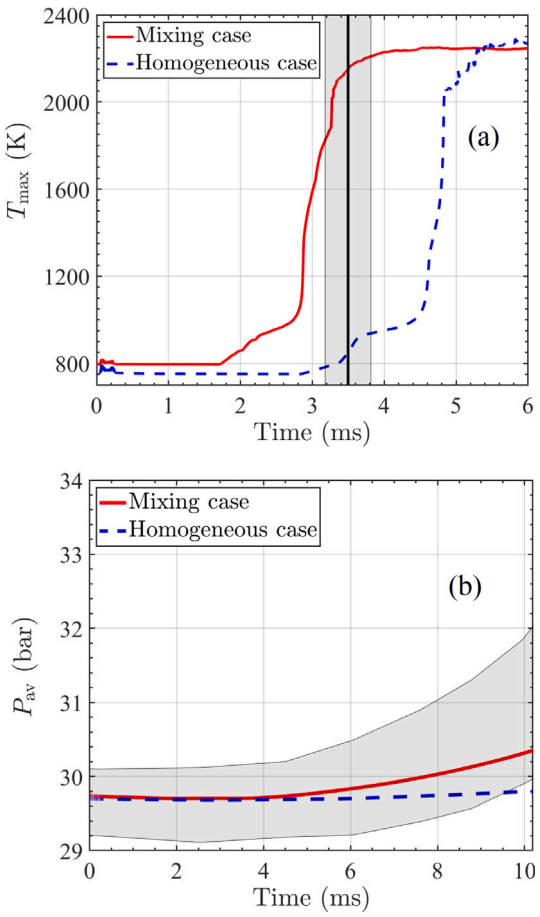

Fig. 7. Validation of the ignition process after methane mixing simulation (Mixing case) and comparing the results with homogeneous case: (a) temporal evolution of maximum temperature (T_{max}). The black solid line and gray shaded area specify the average and error bar of the measured IDT [6], and (b) comparison of numerical and experimental average pressure (P_{av}) of the constant volume combustion chamber as a function of time after the start of pilot diesel injection. The gray shaded area in (b) specifies the error bar of the measured average pressure.

therefore, the definition of the maximum mixture temperature of 2000 K (T_{max} > 2000 K) is used in the next sections.

Two different cases are compared in Fig. 7. In one case (Homogeneous case), pilot diesel fuel is injected into methane and temperature fields that are homogeneous (i.e. no modeling of the methane gas injection is considered). In the other case (Mixing case), pilot diesel fuel is injected into a methane and temperature field that corresponds to Fig. 6, where the modeling of methane gas injection is considered.

The relative error of the simulated IDT to the measured IDT [6] is approximately 7%, and 38% for the mixing case and homogeneous case, respectively (cf. Fig. 7a). This suggests the importance of methane mixing modeling in the simulation of premixed micro-pilot dual-fuel combustion. As shown in Fig. 7b, there is a reasonable agreement between the measured and calculated values for average pressure (P_{av}) after the ignition. It is also shown that there is a large deviation between the predicted P_{av} for the homogeneous case and experimental data. Hence, these results demonstrate that the ignition characteristics of pilot diesel in a premixed methane/air charge is captured when the inhomogeneities are taken into account.

It is worth mentioning that another reduced n-dodecane mechanism developed by Yao et al. [31] was also tested under this operating condition for the mixing case. It is observed that no ignition is captured with Yao mechanism. It is noteworthy that Yao mechanism was shown to ignite in another premixed DF configuration [14], but at a higher ambient temperature (900 K) and density (22.8 kg/m^3), as well as having longer diesel fuel injection duration (i.e. larger amount of injected diesel). However, under the current operating condition with a micro-pilot diesel injection, there is no sign of ignition when the Yao mechanism is used.

Formation and development of the low-temperature (LT) reactions and high-temperature (HT) reactions are examined in detail for the mixing case in order to provide more insights into the ignition characteristics of the pilot fuel. This is carried out to specify the regions with a higher tendency for the occurrence of LT and HT reactions. Formaldehyde (CH_2O) and hydroxyl (OH) radicals are used as indicators of the LT and HT reactions [32], respectively. Fig. 8a shows the spatial distribution of CH_2O and OH, while Fig. 8b depicts the scatter plots of temperature-equivalence ratio ($T - \phi$) colored by CH_2O and OH. Distribution of CH_2O and OH mass as a function of T and ϕ are presented in Fig. 8c. In the CH_2O mass plot, 2 ms is also presented which is around the start of CH_2O formation and after LT ignition start (not shown in Fig. 8a). The equivalence ratio including exhaust gas recirculation is defined based on the formulation in Ref. [33].

At 2 ms, CH_2O exhibits a peak at around T = 780 K and ϕ = 1.0 (Fig. 8c). Meanwhile, OH is not formed during this time, hence indicating the absence of HT reactions. At 3.4 ms, which is around IDT and the start of HT reactions, there is a large region of CH_2O downstream of each pilot diesel jet (Fig. 8a). Fig. 8c shows that the CH_2O at t = 3.4 ms spans a wide range of ϕ values from 0.7 to 1.5, but the peak value is in the fuel-lean region where ϕ = 0.8. It should be mentioned that diesel injection is already finished before this time.

HT ignition sites (represented by OH) start to appear at different locations (indicated by red arrows in Fig. 8a). OH formation starts in regions close to the stoichiometric condition (ϕ = 1), as shown in Fig. 8b and c. At 4 ms the number of ignition sites increases (Fig. 8a) and peak OH mass is found to move toward fuel-lean mixtures (Fig. 8b). After 6 ms, the local high concentration regions of CH_2O start to diminish. The HT reactions continue to develop and peak values of OH move to the fuel-leaner side (Fig. 8c).

As it can be seen from Fig. 8b, due to the mixing process, the pilot diesel rapidly becomes overly fuel-lean, and scatter points move to the lean region. In the micro-pilot DF combustion the injection timing of the pilot diesel is short (0.25 ms in this study). Therefore, the injected diesel mixes with air and rapidly becomes overly fuel-lean.

To further elaborate, the normalized mass of the fuel-rich region (ϕ > 1) is presented in Fig. 9. It can be seen from this figure that as time progresses, the mass of rich region decreases rapidly. The mass of the fuel-rich region decreases by 95% from 2 ms (which is around the start of LT reactions) to 8 ms. Mass distribution plots of OH (Fig. 8c) shows that under the studied operating conditions, high-temperature reactions start around the fuel-rich region close to the stoichiometric condition which is more desirable for these reactions.

4.3. Effect of inhomogeneities on the ignition process

It is observed in the previous section that the inhomogeneities are important for modeling the auto-ignition process of the micro-pilot dual-fuel combustion. However, it is difficult to examine which inhomogeneity parameter (methane or temperature distribution) plays a more dominant role in affecting the auto-ignition process. Therefore, in this section, systematic idealized inhomogeneities for both the methane distribution and temperature distribution are considered inside the CVCC. This allows the possibility to isolate the sensitivity of the predicted IDT to the inhomogeneity in methane and temperature distribution. A sinusoidal distribution is utilized for both methane and temperature. The formulation of the sinusoidal temperature and methane distribution are as follows:

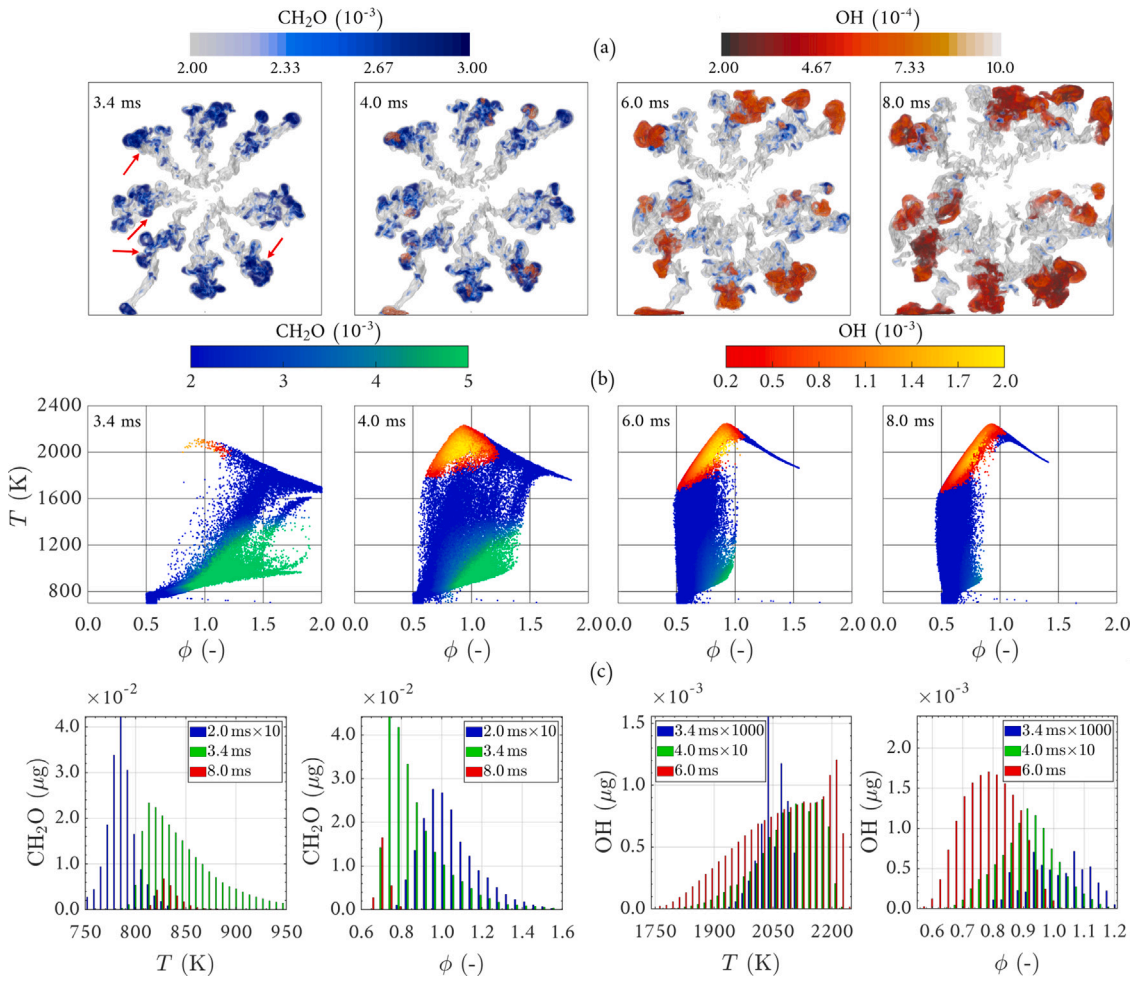

Fig. 8. Formation and development of the low-temperature and high-temperature reactions: (a) Spatial distribution of CH_2O (low-temperature reactions) and OH (high-temperature reactions) at different time instances after the start of pilot diesel injection. The gray iso-surface specifies the diesel cloud. Red arrows show the locations of OH formation, (b) scatter plots of temperature-equivalence ratio ($T-\phi$) at the same time instances as (a), and (c) distribution of CH_2O and OH mass as a function of temperature (T) and equivalence ratio (ϕ). (For interpretation of the references to color in this figure legend, the reader is referred to the web version of this article.)

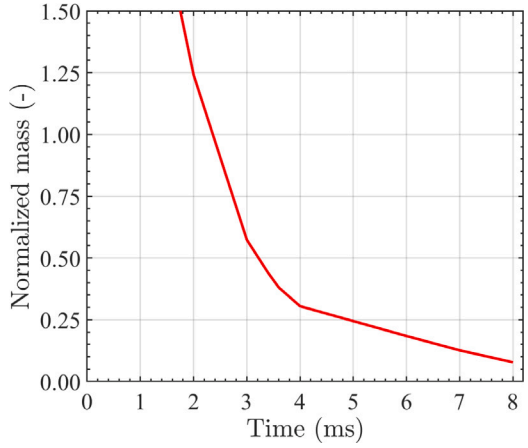

Fig. 9. Mass of fuel-rich region ($\phi > 1$) normalized by the total mass of chamber as a function of time after the start of pilot diesel injection.

$$T(x,y,z) = T_{av} - \frac{A_T}{3}\left(\sin\left(\frac{2\pi x}{\lambda}\right) + \sin\left(\frac{2\pi y}{\lambda}\right) + \sin\left(\frac{2\pi z}{\lambda}\right)\right) \quad (2)$$

$$F(x,y,z) = F_{av} - \frac{A_F}{3}\left(\sin\left(\frac{2\pi x}{\lambda}\right) + \sin\left(\frac{2\pi y}{\lambda}\right) + \sin\left(\frac{2\pi z}{\lambda}\right)\right) \quad (3)$$

where, T_{av} and F_{av} are the average temperature and average methane mole fraction, respectively. A_T and A_F are the amplitudes of the variation from average temperature and average methane mole fraction, respectively. Finally, λ is the wavelength of sinusoidal inhomogeneity distribution. An average value of 31 mm is considered here for the wavelength which is calculated based on mixing simulation results. A similar formula is used to define methane inhomogeneities.

Four different inhomogeneities are considered and their results are compared. Among these cases, two cases represent the inhomogeneity of methane concentration, while the other two cases represent the inhomogeneity of temperature. In all of the cases, the average temperature (T_{av}) and methane molar fraction (F_{av}) are set to 750 K and 4.6%, respectively. These values are the same as those in the homogeneous case, as well as that reported in [6]. The amplitude of the variation in these cases are as follows. $A_F = 10$ represents ±10% variation from the average methane concentration, $A_F = 20$ represents ±20% variation from the average methane concentration, $A_T = 25$ represents ±25 K variation from the average temperature, and $A_T = 50$ represents ±50 K variation from the average temperature. It should be mentioned that the considered levels of inhomogeneity in the methane concentration and temperature are within the ranges that are observed in the simulation of methane/air mixing presented earlier in Section 4.1.

The comparison of the predicted maximum temperature (T_{max}) and average pressure difference (ΔP_{av}) of the CVCC for different cases of

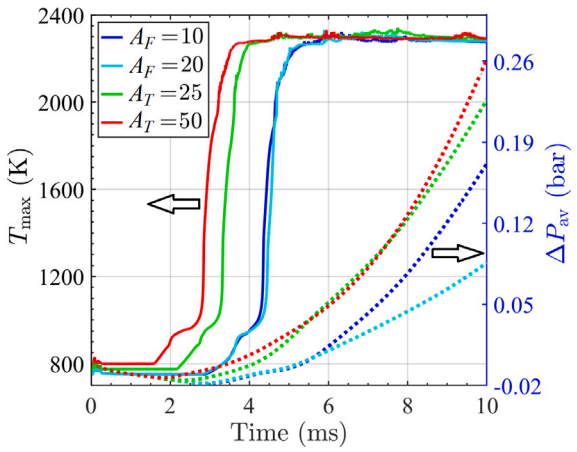

Fig. 10. Temporal evolution of maximum temperature (T_{max}) in solid lines and average pressure difference (ΔP_{av}) in dashed lines as a function of time after the start of pilot diesel injection. A_F and A_T represent the amplitude of inhomogeneity in fuel and temperature, respectively.

Table 1
The low-temperature (τ_1) and high-temperature (τ_2) ignition for different cases of inhomogeneity and the time lapse ($\tau_2 - \tau_1$) between these stages. IDT and τ_2 have the same values. A_F and A_T represent the amplitude of inhomogeneity in fuel and temperature, respectively.

Case	(A_F, A_T)	τ_1 (ms)	τ_2 (ms)	$\tau_2 - \tau_1$ (ms)
A_F = 10	(10%, 0 K)	2.28	4.65	2.37
A_F = 20	(20%, 0 K)	2.27	4.68	2.44
A_T = 25	(0%, 25 K)	1.61	3.62	2.01
A_T = 50	(0%, 50 K)	1.29	3.22	1.93

inhomogeneity is presented in Fig. 10. ΔP_{av} presents the difference between the temporal evolution of the average pressure of the CVCC and the average pressure of the CVCC at the start of pilot diesel injection. The predicted IDT values for different cases are also reported in Table 1. Based on Fig. 10 and Table 1, inhomogeneity in methane distribution does not change the IDT considerably. On the other hand, the inhomogeneity in the temperature has a considerable influence on the predicted IDT. When examining the ΔP_{av}, both variations of methane and temperature distribution have a significant effect (Fig. 10). Especially, in the $A_F = 20$ case, the low values of ΔP_{av} at later time instances (time > 6 ms) is a sign of poor combustion for this case which will be discussed later. The negative values of ΔP_{av} for all the cases are due to the reduction of average pressure compared to P_{av} value at the start of pilot injection. These negative values are more pronounced for the cases with methane inhomogeneity due to longer ignition delay and later start of combustion. Overall, inhomogeneity not only changes local parameters (T_{max}), but also varies the global parameters (P_{av}).

Fig. 11 shows the temporal evolution of the maximum and average mass fraction of CH_2O (Fig. 11a) and OH (Fig. 11b) for different cases of inhomogeneity. The start of CH_2O formation indicates the low-temperature (LT) ignition (τ_1) and the start of OH formation specifies the high-temperature (HT) ignition (τ_2). The predicted values for τ_1 and τ_2 and the time lapse between them are shown in Table 1. Based on the results, the start of LT ignition is not affected by the inhomogeneity in the methane distribution as the start time of CH_2O formation for the cases with 10% and 20% inhomogeneity in methane (A_F = 10 and A_F = 20) are almost the same. However, the average value of CH_2O (Fig. 11a) for the $A_F = 20$ case continuously increases. This means this radical does not undergo HT reactions and therefore, there is a difference between the cases with different inhomogeneity levels in methane concentration in the combustion phase and flame development.

In contrast, temperature inhomogeneity has a considerable effect on LT ignition. The HT ignition also shows a similar trend as the LT ignition with temperature inhomogeneity. Based on 0D homogeneous reactor tests, the shortest high-temperature IDT for methane-diesel DF combustion occurs in the mixtures with slightly fuel-rich regions [4,5]. Furthermore, the results of OH mass distribution at 3.4 ms in Fig. 8c suggest the tendency of HT reactions occurring around the slightly fuel-rich regions. As discussed previously, in the micro-pilot DF combustion, the pilot fuel/air mixture rapidly becomes overly fuel-lean due to the short injection timing of the pilot fuel (cf. Fig. 9). Therefore, any delay in the start of the reaction chain (τ_1) leads to a longer time for pilot fuel mixing and hence leaner mixtures of the pilot fuel/air which results in less likely initiation of HT reactions and longer IDTs.

Also, considering the same value of equivalence ratio for pilot diesel, increasing the ambient methane concentration increases the IDT significantly [5,8]. Therefore, higher concentrations of methane in the ambient are not in favor of the formation of ignition kernels. This can explain why the average pressure difference (Fig. 10) and average OH (Fig. 11a) are lower for $A_F = 20$ case than that for $A_F = 10$ case.

To further elaborate, Fig. 12 shows the spatial distribution of CH_2O and OH for the case with variation in fuel concentration ($A_F = 20$, where $A_F = 20\%$, $A_T = 0$ K) and the case with variation in temperature ($A_T = 50$, where $A_F = 0\%$, $A_T = 50$ K). As it can be seen, for $A_F = 20$ case, even in the later time instances as 10 ms after diesel SOI, some of the diesel jets are still not ignited. Furthermore, the size of the ignition kernels for the $A_F = 20$ case is much smaller than that in the $A_T = 50$ case in the same time instances. This leads to a lower combustion rate for the $A_F = 20$ case.

4.4. Effect of inhomogeneities wavelength on the ignition process

In this section, the effect of the wavelength (λ) of the idealized inhomogeneities is studied on the ignition process. Wavelength (λ) which is shown in Eqs. 2 and 3 is the spatial distance over which the sinusoidal wave's shape repeats. As mentioned before, the average value of 31 mm is considered for wavelength in the previous section. This value represents the average wavelength of all inhomogeneities in the domain. However, it can be seen from Fig. 6 that different sizes of inhomogeneities are distributed inside the domain before the pilot diesel SOI. Therefore, a sensitivity analysis is carried out to check the effect of λ on the ignition process. Three different values are considered for λ, including 21 mm, 31 mm, and 41 mm. In all three cases, a temperature inhomogeneity of $A_T = 50$ K is considered before pilot diesel injection.

The comparison of the predicted maximum temperature and average pressure difference of the CVCC for different values of wavelength is presented in Fig. 13a. As can be seen, increasing the wavelength leads to a reduction of IDT. Furthermore, for the larger wavelength case (λ = 41 mm), the average pressure difference (ΔP_{av}) increases more than the other cases. This is suggesting a higher combustion rate for the λ = 41 mm case than the others. To study the influence of inhomogeneity wavelength on LT and HT reactions, the average mass fraction of CH_2O and OH are presented in Fig. 13b. The onset of the LT ignition delay is delayed for λ = 21 mm. However, all of the cases follow the same trend. On the other hand, the HT reactions show a considerable variation by changing the wavelength which is similar to the average pressure difference trend that is shown in Fig. 13a.

After the end of the pilot diesel injection, the cloud of diesel from each nozzle hole propagates inside the chamber. This cloud passes through the different local inhomogeneities. The higher combustion rate for larger values of wavelength is probably due to larger regions of inhomogeneity with the desirable condition for flame development. Therefore, the presence of diesel jets in the high-temperature region for a longer time that leads to combustion enhancement.

To gain more insights into this, Fig. 14 shows the spatial distribution of CH_2O and OH for different values of inhomogeneity wavelength at 10 ms after pilot diesel SOI. As can be seen, in the $\lambda = 21$ mm case, the ignition kernels are weak and small. This suggests that, in the small

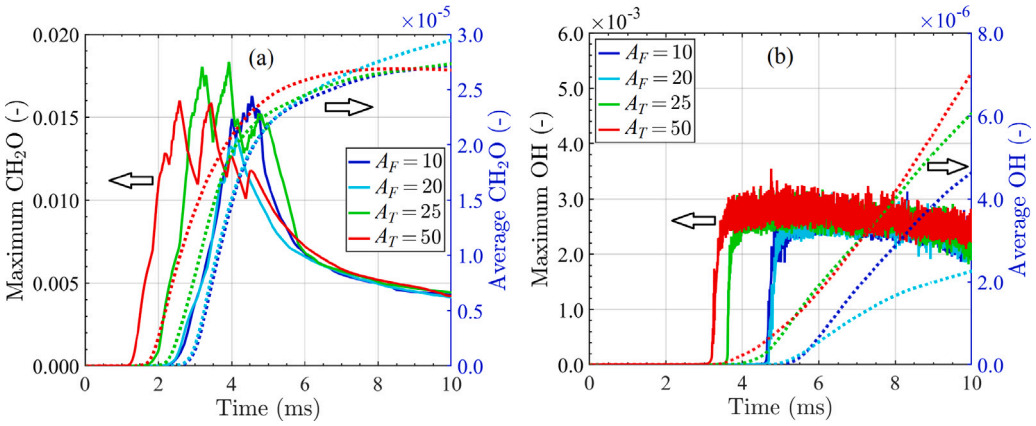

Fig. 11. Temporal evolution of (a) maximum (solid) and average (dashed) mass fraction of CH_2O and (b) maximum (solid) and average (dashed) mass fraction of OH as a function of time after the start of pilot diesel injection for different cases of inhomogeneity. A_F and A_T represent the inhomogeneity in fuel and temperature, respectively.

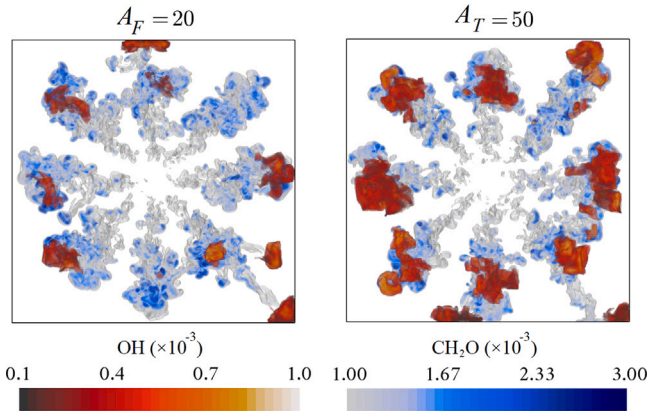

Fig. 12. Spatial distribution of CH_2O and OH for the case with inhomogeneity of methane distribution (A_F = 20: A_F = 20%, A_T = 0 K) and the case with inhomogeneity in temperature distribution (A_T = 50: A_F = 0%, A_T = 50 K) at 10 ms after the start of pilot diesel injection. The gray iso-surface specifies the diesel cloud.

wavelengths (λ = 21 mm), the fuel jets pass through the local high-temperature locations before they heat up sufficiently and combust. A very small wavelength can be considered similar to a homogeneous case. While in the larger wavelength case (λ = 41 mm), the ignition kernels are strong which leads to a higher combustion rate. In the λ = 41 mm case, some of the fuel jets have not ignited properly as they pass through the local low-temperature regions.

5. Conclusion

In the present work, the auto-ignition process of a premixed micro-pilot diesel-methane dual-fuel (DF) combustion is investigated in a constant volume combustion chamber by performing large eddy simulations (LES). The present LES is able to predict the pressure variation during the methane mixing process. More importantly, it is able to capture the ignition delay time (IDT) to be within a maximum relative difference of 7% as compared to measurements. Simulation of the methane injection and mixing process shows that there are pockets of inhomogeneity in both methane and temperature distribution before the pilot diesel injection. It is also observed that under the studied operating conditions, the high-temperature reactions start around the fuel-rich region close to the stoichiometric condition.

A higher relative difference of 38% is obtained when methane gas injection is omitted and the methane/air is assumed homogeneous. This demonstrates the importance of inhomogeneities caused by methane gas injection. It is found that the the temperature inhomogeneity advances the low-temperature ignition and, subsequently, the high-temperature ignition (IDT), considerably. However, in the cases with inhomogeneous methane distribution, low-temperature ignition is delayed. Meanwhile, the pilot fuel/air mixture becomes overly fuel-lean rapidly due to the short injection duration and low amount of pilot fuel. These two coupling effects ultimately lead to an overall longer IDT of the pilot fuel and weaker ignition kernels (or lower number of ignition sites) which results in lower combustion rates. A sensitivity analysis on the effect of inhomogeneity wavelength reveals that the larger wavelengths enhance the combustion due to the longer residence time of the pilot diesel jet within the region desirable for combustion to occur.

This work highlights the importance of the mixing process modeling in the simulation of premixed DF combustion, and also the levels of inhomogeneity that need careful attention in the auto-ignition prediction of micro-pilot premixed DF.

CRediT authorship contribution statement

Arash Nemati: Conceptualization, Formal analysis, Funding acquisition, Investigation, Methodology, Software, Validation, Writing – original draft. **Jiun Cai Ong:** Conceptualization, Supervision, Validation, Writing – review & editing, . **Min Zhang:** Investigation, Writing – review & editing. **Jens Honoré Walther:** Conceptualization, Funding acquisition, Resources, Supervision, Writing – review & editing.

Declaration of competing interest

The authors declare that they have no known competing financial interests or personal relationships that could have appeared to influence the work reported in this paper.

Data availability

The authors are unable or have chosen not to specify which data has been used.

Acknowledgments

The authors gratefully acknowledge the financial support from The Danish Maritime Fund (DDMF) under the grant number 2021-080. The computations were performed using the Niflheim cluster at the Technical University of Denmark (DTU). The authors acknowledged PRACE for awarding us access to Joliot-Curie at GENCI@CEA, France.

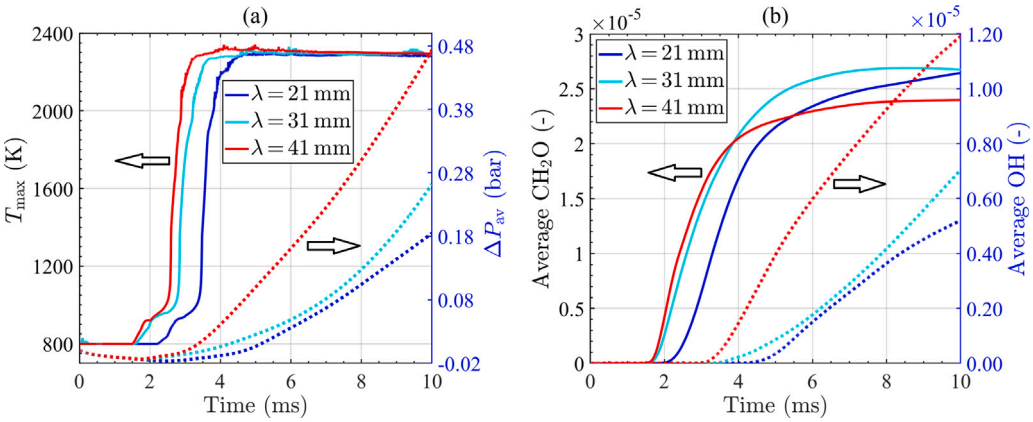

Fig. 13. Temporal evolution of (a) maximum temperature (T_{max}) in solid lines and average pressure difference (ΔP_{av}) in dashed lines and (b) average CH_2O (solid) and average OH (dashed) mass fraction as a function of time after the start of pilot diesel injection for different cases of inhomogeneity wavelength (λ).

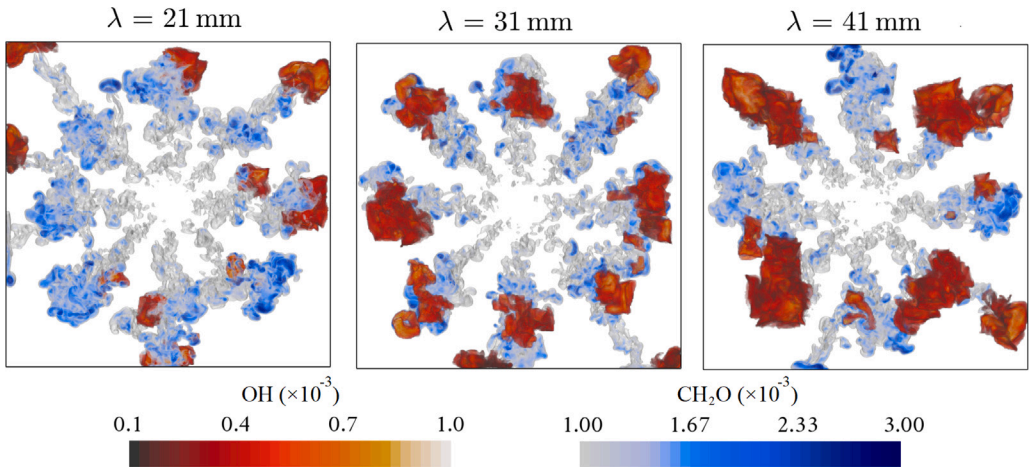

Fig. 14. Spatial distribution of CH_2O and OH for different inhomogeneity wavelengths (λ) at 10 ms after the start of pilot diesel injection. The gray iso-surface specifies the diesel cloud.

References

[1] Liu J, Yang F, Wang H, Ouyang M, Hao S. Effects of pilot fuel quantity on the emissions characteristics of a CNG/diesel dual fuel engine with optimized pilot injection timing. Appl Energy 2013;110:201–6.

[2] Nemati A, Ong JC, Pang KM, Mayer S, Walther JH. A numerical study of the influence of pilot fuel injection timing on combustion and emission formation under two-stroke dual-fuel marine engine-like conditions. Fuel 2022;312:122651.

[3] Srna A, Bruneaux G, Von Rotz B, Bombach R. Optical investigation of sooting propensity of n-dodecane pilot/lean-premixed methane dual-fuel combustion in a rapid compression-expansion machine. SAE Int J Engines 2018;11(6):1049–68.

[4] Srna A, Bolla M, Wright YM, Herrmann K, Bombach R, Pandurangi SS, Boulouchos K, Bruneaux G. Effect of methane on pilot-fuel auto-ignition in dual-fuel engines. Proc Combust Inst 2019;37(4):4741–9.

[5] Srna A, von Rotz B, Bolla M, Wright YM, Herrmann K, Boulouchos K, Bruneaux G. Experimental investigation of pilot-fuel combustion in dual-fuel engines, Part 2: Understanding the underlying mechanisms by means of optical diagnostics. Fuel 2019;255:115766.

[6] Yang X, Vinhaes VB, Turcios M, McTaggart-Cowan G, Huang J, Naber J, Shahbakhti M, Schmidt H, Atkinson W. Process for study of micro-pilot diesel-NG dual fuel combustion in a constant volume combustion vessel utilizing the premixed pre-burn procedure. SAE Tech. Paper Ser. 2019–01–1160, 2019.

[7] Rajasegar R, Niki Y, Garcia-Oliver JM, Li Z, Musculus M. Spatio-Temporal progression of two-stage autoignition for diesel sprays in a low-reactivity ambient: n-heptane pilot-ignited premixed natural gas. SAE Technical Paper 2021-01-0525, 2021.

[8] Niki Y, Rajasegar R, Li Z, Musculus MP, Garcia Oliver JM, Takasaki K. Verification of diesel spray ignition phenomenon in dual-fuel diesel-piloted premixed natural gas engine. Int J Engine Res 2020;1468087420983060.

[9] Grochowina M, Schiffner M, Tartsch S, Sattelmayer T. Influence of injection parameters and operating conditions on ignition and combustion in dual-fuel engines. J Eng Gas Turbines Power 2018;140(10).

[10] Grochowina M, Hertel D, Tartsch S, Sattelmayer T. Ignition of diesel pilot fuel in dual-fuel engines. J Eng Gas Turbines Power 2019;141(8).

[11] Cheng Q, Ahmad Z, Kaario O, Martti L. Cycle-to-cycle variations of dual-fuel combustion in an optically accessible engine. Appl Energy 2019;254:113611.

[12] Wei H, Qi J, Zhou L, Zhao W, Shu G. Ignition characteristics of methane/n-heptane fuel blends under engine-like conditions. Energy Fuels 2018;32(5):6264–77.

[13] Zhao W, Zhou L, Liu Z, Qi J, Lu Z, Wei H, Shu G. Numerical study on the combustion process of n-heptane spray flame in methane environment using large eddy simulation. Combust Sci Tech 2021;193(1):142–66.

[14] Kahila H, Kaario O, Ahmad Z, Masouleh MG, Tekgül B, Larmi M, Vuorinen V. A large-eddy simulation study on the influence of diesel pilot spray quantity on methane-air flame initiation. Combust Flame 2019;206:506–21.

[15] Tekgül B, Kahila H, Kaario O, Vuorinen V. Large-eddy simulation of dual-fuel spray ignition at different ambient temperatures. Combust Flame 2020;215:51–65.

[16] Engine combustion network. 2021, available from: https://ecn.sandia.gov/.

[17] Kilic AK, Köysüren S, Ong JC, Nemati A, Walther JH. Numerical simulation of a premixed dual-fuel combustion in a constant volume combustion chamber. In: HEFAT 2021, 15th international conference on heat transfer, fluid mechanics and thermodynamics. Prague, Czech Republic: HEFAT; 2021.

[18] Ong JC, Zhang M, Jensen MS, Walther JH. Large eddy simulation of soot formation in ducted fuel injection configuration. Fuel 2022;131:122735.

[19] Nemati A, Barzegar R, Khalilarya S. The effects of injected fuel temperature on exergy balance under the various operating loads in a DI diesel engine. International Journal of Exergy 2015;17:35–53.

[20] Zhang M, Ong JC, Pang KM, Bai X-S, Walther JH. An investigation on early evolution of soot in *n*-dodecane spray combustion using large eddy simulation. Fuel 2021;293:120072. http://dx.doi.org/10.1016/j.fuel.2020.120072.

[21] Nemati A, Ong JC, Walther JH. CFD analysis of combustion and emission formation using URANS and LES under large two-stroke marine engine-like conditions. Appl Thermal Engng 2022;216:119037.

[22] Germano M, Piomelli U, Moin P, Cabot WH. A dynamic subgrid-scale eddy viscosity model. Phys Fluids 1991;3:1760–5.
[23] Nemati A, Ong JC, Jensen MV, Pang KM, Mayer S, Walther JH. Numerical study of the scavenging process in a large two-stroke marine engine using URANS and LES turbulence models. SAE Tech. Paper Ser. 2020-01-2012, 2020, http://dx.doi.org/10.4271/2020-01-2012.
[24] Reitz RD, Diwakar R. Effect of drop breakup on fuel sprays. SAE Tech. Paper Ser. 860469, 1986, p. 1–10.
[25] Nemati A, Jensen MV, Pang KM, Walther JH. Conjugate heat transfer simulation of sulfuric acid condensation in a large two-stroke marine engine - the effect of thermal initial condition. Appl Thermal Engng 2021;195:117075.
[26] Lapointe S. Lawrence livermore national laboratory, n-dodecane hybrid mechanism. 2019, https://combustion.llnl.gov/mechanisms/alkanes/n-dodecane, accessed: 2020-10-01.
[27] Naber JD, Henes R, Henes E. High BMEP and high efficiency micro-pilot ignition natural gas engine (Final Project Report). Project report, Houghton, MI (United States): Michigan Technological Univ; 2020.
[28] Celik IB, Cehreli ZN, Yavuz I. Index of resolution quality for large eddy simulations. J Fluids Engng 2005;127:949–58.
[29] Srna A, von Rotz B, Herrmann K, Boulouchos K, Bruneaux G. Experimental investigation of pilot-fuel combustion in dual-fuel engines, Part 1: Thermodynamic analysis of combustion phenomena. Fuel 2019;255:115642.
[30] Pang KM, Jangi M, Bai X-S, Schramm J. Evaluation and optimization of phenomenological multi-step soot model for spray combustion under diesel engine-like operating conditions. Combust Theory Model 2015;19(3):279–308.
[31] Yao T, Pei Y, Zhong B-J, Som S, Lu T, Luo KH. A compact skeletal mechanism for n-dodecane with optimized semi-global low-temperature chemistry for diesel engine simulations. Fuel 2017;191:339–49.
[32] Dahms RN, Paczko GA, Skeen SA, Pickett LM. Understanding the ignition mechanism of high-pressure spray flames. Proc Comb Inst 2017;36(2):2615–23.
[33] Xu L, Bai X-S, Li C, Tunestål P, Tunér M, Lu X. Combustion characteristics of gasoline DICI engine in the transition from HCCI to PPC: Experiment and numerical analysis. 2019;185:922–37.